Chemical Engineering Journal 160 (2010) 814–822

Contents lists available at ScienceDirect

Chemical Engineering Journal

journal homepage: www.elsevier.com/locate/cej

Thermal analysis of chemical reaction with a continuous microfluidic calorimeter

Cindy Hany[a,*], Helene Lebrun[a], Christophe Pradere[b], Jean Toutain[b], Jean-Christophe Batsale[b]

[a] LOF, Université Bordeaux 1, UMR CNRS-Rhodia-UB1 5258,178 avenue du docteur Schweitzer, 33608 Pessac, France
[b] TREFLE, Université Bordeaux 1, UMR 8508 CNRS-ENSAM-UB1, Esplanade des Arts et Métiers, 33405 Talence, France

ARTICLE INFO

Article history:
Received 10 July 2009
Received in revised form 22 February 2010
Accepted 24 February 2010

Keywords:
Microfluidic
Thermal and chemical analysis
Flow microcalorimeter
Enthalpy

ABSTRACT

This paper presents a continuous microfluidic calorimeter to measure kinetics and enthalpy of very dangerous, highly exothermic chemical reactions. The main idea is to use a microfluidic chip, in co-flow or droplet flow, where the microchannel acts as the chemical reactor. A thermopile (Peltier element) measures the global heat flux dissipated during the chemical reaction. A highly thermal conductive plate is placed between the thermopile and the reactor to avoid severe temperature gradients and to let most of the heat flux go through this plate. Because of the microchannel dimensions only a small amount of products is required.

1. Introduction

The kinetics and the thermodynamics of chemical reactions are important features for the development and the safety of chemical processes. It is well known that both heat transfer and chemical kinetics occur during chemical reactions and that one way to control and to measure those phenomena is by calorimetry. Therefore the characterization of exothermic chemical reactions is well developed in the literature and different types of calorimeters already exist [1].

The recent development of MEMS (Micro-Electro-Mechanical Systems) provides a very promising range of new tools to characterize chemical reactions in continuous flow at a small scale. The main advantage of those systems is the small size of the microchannels which permits the controlled mixing of the reactants. Indeed, the flow is laminar with low Reynolds number ($\ll$100). It is also convenient to use a small amount of products and to be able to easily and quickly test a large number of chemical reaction configurations [2]. Moreover, the high ratio between surface and volume allows to control the heat transfer and to investigate very exothermic reactions under safe operation conditions. Nevertheless, measurement of the temperature and the heat flux at such a small scale represents the main difficulty.

However to date, several studies address this topic. Most of them use local temperature microsensors which need specific and quite complex design of integrated circuits [3–5]. Lechner et al. have built different integrated circuit calorimeters adapted to characterize enzyme-catalysed reactions [6]. Ross et al. and Arata et al. have developed an intrusive method using a fluorescent dye to measure the temperature distribution inside the microchannel [7,8]. Another method allows to obtain the temperature field of all the microfluidic chip by the mean of an infrared (IR) camera. Möllmann et al. and Antes et al. have proved the IR camera can be used to develop and optimize microsystems [9,10]. The IR thermography has also been used to estimate the reaction enthalpy of a chemical reaction in microsystem by Hany et al. [11].

In this context, we have developed a tool which combines the use of microvolumes, a high thermal sensitivity, a good control of the reagent mixing and of isothermal conditions.

The method applied here measures the global heat flux around the microchannel thanks to a fluxmeter located under the standard microfluidic chip. The main purpose of this paper is to present this new microcalorimeter. In the first part, the experimental device principle is described. An analytical model that describes the thermal behaviour is introduced. The importance of thermal properties of the wafer used for the microfluidic chip is discussed. Furthermore, a thermal calibration (by Joule effect) is performed in order to verify the features of the microcalorimeter. The second part deals with the validation of the microcalorimeter with measurement of the enthalpy of a strong acid–base chemical reaction. Such validation is realised in two flow configurations: co-flow where the two reactants flow side by side through the microchannel and droplet flow where the reactants are contained inside droplets carried by an inert continuous phase. Then, the conversion rate of this chemical

* Corresponding author. Tel.: +33 556464751; fax: +33 556464790.
E-mail address: cindyhany@netcourrier.com (C. Hany).

1385-8947/$ – see front matter © 2010 Elsevier B.V. All rights reserved.
doi:10.1016/j.cej.2010.02.048

reaction can be estimated for different residence times and temperatures. Furthermore, we demonstrate that calorimetric titration experiments are also possible with this simple device. Finally, an esterification reaction is characterized by the determination of the mixing and reaction enthalpy.

2. Microcalorimeter description

2.1. Microcalorimeter design

A differential microcalorimeter has been developed containing two microfluidic chips in two separated chambers (Fig. 1) [12]. One microfluidic chip is used for the reference and the other one to carry out the chemical reaction. Each microfluidic chip is placed above a thermopile used to measure the heat flux. The reagent flow rates are established with a syringe pump (Nemesys). No fluids are injected in the reference chip which is used as baseline.

Both microfluidic chips are built with a PDMS (PolyDiMethylSiloxane) matrix, containing a negative channel network. This PDMS matrix is glued onto silicon wafer after UV–ozone activation. Since silicon is a good thermal conductor, the chemical reaction occurs under isothermal conditions in the microchannel. PDMS has been chosen because it is usually employed to realise microfluidic chip, it is easy to use and allows to obtain various channel geometries. Moreover, PDMS is good insulator that is necessary in our device (cf. Section 2.2). However, it is not an inert material and some interactions can occur with some solvents. The selected substrate (thickness 500 μm) is made of silicon with a 5 cm diameter.

The microfluidic channel is 32 cm long, 250 μm wide and 250 μm high. The channel is a serpentine channel to optimize the volume of the chip.

The voltage is measured with thermopiles (3) by Seebeck effect. The voltage obtained from the reference chamber (1r) is substracted to the voltage from the reaction one (1). Then, by using the calibration coefficient (cf. Section 2.3) the heat flux produced by the chemical reaction can be determined.

The calorimetric sensitive area is a 50 mm × 50 mm square (four thermopiles connected in series). The voltage is measured with a numerical voltmeter (Agilent 34970 A). The temperature (Ts) is set by a thermostatic flow circulation (5). A computer using Labview™ software controls all these steps via a RS232 port.

In order to minimize perturbations of the baseline caused by the environmental thermal variations, the thermopiles are placed on a brass block (4) of 20 cm × 20 cm × 2.5 cm used as an isothermal reservoir. Due to the high thermal capacity of the bulk, the variation of the baseline is less than 10 μW on 10 h. There is no influence

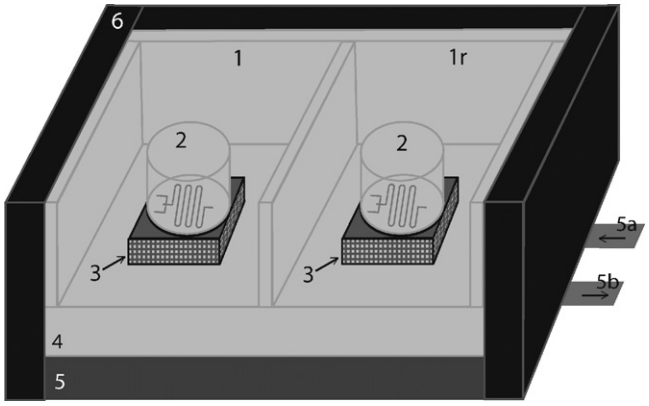

Fig. 1. Scheme of the microcalorimeter: (1) reaction chamber, (1r) reference chamber, (2) microfluidic chip composed of PDMS resin and silicon wafer, (3) thermopile with ceramic plates and thermoelectric elements, (4) isothermal brass block, (5) stainless plate, (5a and 5b) thermostatic flow circulation, and (6) insulating foam.

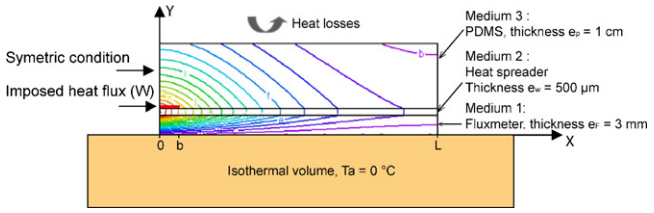

Fig. 2. Representation of the semi infinite thermal problem when a heat flux of 1 W is imposed.

of the baseline on the experiment for several reasons: the measured voltage is a differential measurement, the experiment time is shorter than 10 h.

Then a stainless plate (5) is put below the brass block. This plate is thermally regulated via a thermostatic flow circulation from Ts = 5 to 90 °C. This allows to perform experiments at various temperatures depending on the fluid properties. All parts of the calorimeter are heat shielded by insulating foam (6). Furthermore, the inlet fluid is preheated by passing through the brass block via a groove allowing to fix the tubing. As a result, the chemical reaction begins in the microcalorimeter at the setting temperature (Ts).

2.2. Thermal modeling of the microfluidic chip

In order to model the thermal behaviour of the microfluidic chip, a 2D transient thermal problem (Fig. 2) is considered. The system is made of three homogeneous media of different thermal properties: medium 1 is the thermopile used as fluxmeter, medium 2 is the wafer of the microfluidic chip and medium 3 is the elastomeric PDMS where the microchannels for chemical reaction are imprinted.

The 2D transient model, described by Eq. (1) allows to calculate the temperature field in the different media of the microfluidic chip when a chemical heat flux is generated in the microreactor (Fig. 2).

$$\frac{\partial^2 T_i}{\partial x^2} + \frac{\partial^2 T_i}{\partial y^2} = \frac{1}{a_i}\frac{\partial T_i}{\partial t}, \quad i = 1, 2 \text{ or } 3 \quad \text{and} \quad a_i = \frac{\lambda_i}{\rho_i c_{p,i}} \tag{1}$$

where i is the subscript of each media, T is the temperature (K), a is the thermal diffusivity ($m^2\ s^{-1}$), λ is the thermal conductivity ($W\ m^{-1}\ K^{-1}$), ρ is the mass density ($kg\ m^{-3}$) and C_p the heat capacity ($J\ kg^{-1}\ K^{-1}$).

First, we assume that the chemical heat flux can be represented as a discontinuous function $\Phi(x, t)$ along the plate whose value is zero for x greater than the length b and positive for x between 0 and b (Eq. (2)).

$$\Phi(x,t) = \begin{cases} QH(t) & \text{if} \quad 0 < x \le b \\ 0 & \text{if} \quad b < x < L \end{cases} \tag{2}$$

where Q is the heat flux (W), H is the Heaviside step function and b is the width of the thermal flux (m). Then, we suppose that the media are semi infinite in the x direction. We also assume that heat losses by convection are located at the top of the elastomeric PDMS. Finally, the thermal reservoir positioned at the base of the fluxmeter allows to impose a well known temperature (Ts) on the calorimeter.

The model described above is solved by the quadrupole method [13,14]. With this simple analytic model, it is possible to accurately analyse the thermal heat transfer in the microfluidic chip. The thermal properties of the chip wafer and its size are very important to design the chip properly. Usually, glass or silicon wafers are used. Fig. 3 shows the effect of the thermal properties of the wafer on the microreactor temperature when a heat flux of a 1 W is dissipated through the channel. We have chosen to impose a flux of 1 W because the volume and reagent quantity are very low and the heat flux produced by the chemical reaction will be less than 1 W. We

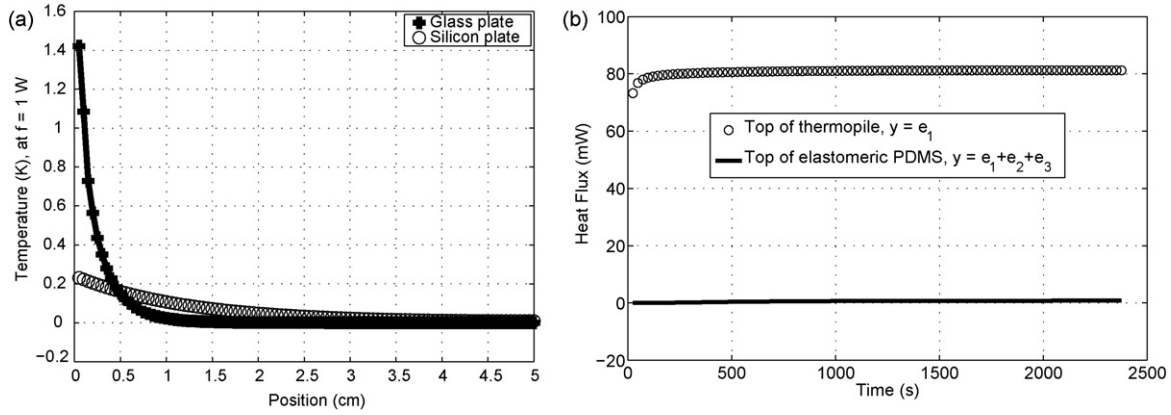

Fig. 3. (a) According to the thermal modelisation the steady state temperature on fluxmeter ($y = e_1$) can be plotted versus the wafer length for glass and silicon wafer of 500 μm thick; thus it is obvious that the local temperature is higher with a glass wafer than with a silicon wafer and (b) the transient heat flux on both thermopile and PDMS layer is represented by a function of time thanks to the thermal modelisation; thus we can see that most of the heat flux goes through the thermopile, and less than 0.01% of the heat flux goes through the PDMS.

can observe in Fig. 3(a) that the maximum temperature variation depends on the wafer. The highest temperature for a glass wafer is about 1.5 K, whereas it is only 250 mK for silicon wafer (6 times smaller). Thus, as the microreactor should be as isothermal as possible, it is better to design the microfluidic chip with the silicon wafer.

Another intention of this analytical model is to study the heat flux distribution in transient conditions. First, the time response of the system is analysed. The heat flux imposed at the top of the silicon plate is still a surface flux ($b = 1$ mm long) and constant in time. The heat flux received both by the fluxmeter and the PDMS layers can be compared, as it is shown in Fig. 3(b).

The heat flux on the thermopile is very important relatively to the flux through the PDMS. The calculation of the percentage ratio, shows that 99% of the heat flux generated by the chemical reaction goes through the silicon. Thus, the fluxmeter placed below the microfluidic chip will detect almost all the heat flux. The heat losses, which represent 1% of the global heat flux, are calibrated using Joule effects.

2.3. Electrical calibration

The tension acquired by the fluxmeter is proportional to a heat flux. According to the data from the supplier, the relation between the heat flux and the tension is given by Eq. (3).

$$\phi = \frac{\lambda G}{\beta} U = \alpha U \quad \text{with} \quad \alpha = \frac{\lambda G}{\beta} \tag{3}$$

where ϕ is the flux (W), λ is the thermal conductivity ($W\,m^{-1}\,K^{-1}$), β is the Seebeck coefficient ($V\,K^{-1}$), G is the shape factor (m) and U is the tension (V).

Thus, the coefficient α, obtained by the data given by the supplier, depends on the properties of the fluxmeter and varies with the temperature (Fig. 4).

It is interesting to compare the calibration coefficient, α, given by the manufacturer with ours. Therefore, we calibrate the microcalorimeter by Joule effect using an electrical heat source. For that purpose, a calibration chip is manufactured with an electrical resistance. This resistance is realised by gold deposition and located between the silicon wafer and the PDMS. This calibration chip is placed inside the reaction part and a microfluidic chip without flow inside the reference part. Various electrical power from 100 mW to 1 W are applied to the system thanks to a power supply (Agilent E3631A) at 25, 50 and 80 °C. Then, the dissipated heat flux is measured by the thermopile as a function of time. For each of them, electrical power was set on, until steady state was reached. Then, the power supply was stopped. For example Fig. 5 illustrates the measured signal while a power of 500 mW is applied.

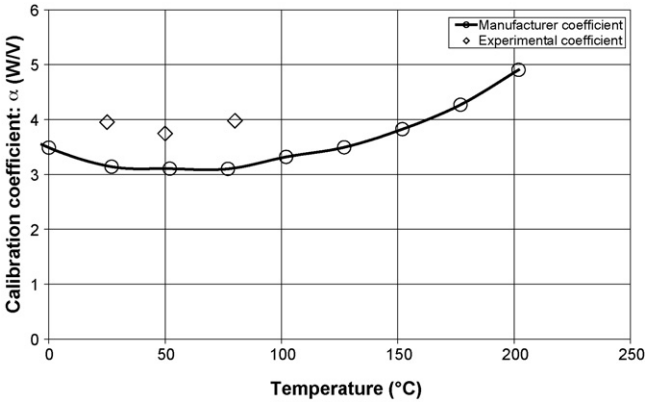

Fig. 4. Manufacturer and experimental calibration coefficient versus temperature.

This procedure allows the measurement of two values of the heat flux, one during the rising part of the response, the other one during the decreasing part. The measured voltage is then compared with the imposed flux (Fig. 6).

From Eq. (3), the calibration coefficient can be determined and we obtain: $\alpha_{25\,°C} = 3.935\,W\,V^{-1}$. Thus, when a chemical reaction occurs in the microcalorimeter, the heat flux is measured in volt

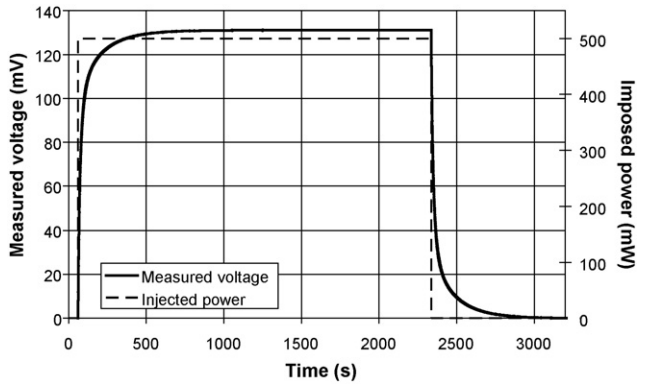

Fig. 5. Heat flux measured and the imposed power are plotted versus time at Ts = 25 °C.

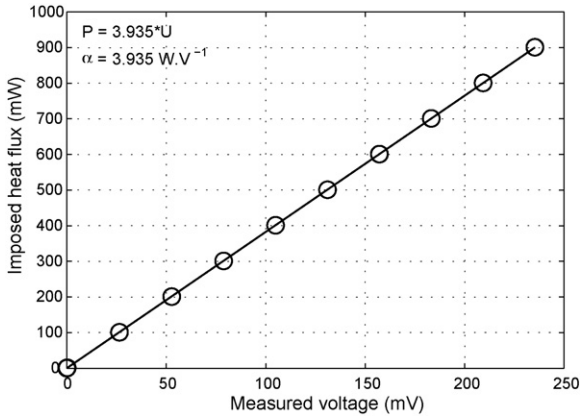

Fig. 6. Imposed heat flux versus measured tension at Ts = 25 °C, the solid line corresponds to the linear regression.

and this coefficient (α) is used to deduce the chemical heat flux (W).

As the thermal conductivity and Seebeck coefficient of the Peltier depend on temperature, the calibration coefficient should be estimated for each temperature we used (Table 1). The experimental coefficients are slightly higher than the manufacturer ones with a proportional coefficient close to 1.25. This difference can be explained by a different way to estimate this coefficient. However, we can observe in Fig. 4 that the evolution of α versus temperature has the same tendency for both the manufacturer and our experimental values.

2.4. Sensitivity

The accuracy of the calibration coefficient is estimated by reproductibility experiments at three different temperatures. The calibration coefficient α is evaluated 30 times for each temperature. The relative error is calculated using the standard deviation of α and Eq. (4).

$$u_\alpha(\%) = \frac{\sigma}{\alpha} 100 \tag{4}$$

where u_α is the relative error of the calibration coefficient (α ($\mathrm{W\,V^{-1}}$)), σ is the standard deviation of the calibration coefficient determined by experiment ($\mathrm{W\,V^{-1}}$). Table 2 presents the results obtained for the different temperatures.

3. Microcalorimeter testing: results and discussion

3.1. Reaction enthalpy measurements

A promising application of microtechnologies is the use of one phase liquid flow (co-flow) or two-phase liquid–liquid flow (droplets flow). In the co-flow configuration the two reactants flow through the microchannel in parallel. In the latter, microdroplets of reagents are transported at constant velocity in an inert continuous phase. Each droplets can be considered as individual nanovolume batch reactors. A very exothermic reaction between a strong acid (HCl) and base (NaOH) is performed for these two flow configurations. The concentrations of the two reactants are 0.2 M. The dimensions of the microfluidic chip given in Section 2.1. The experimental procedure followed during measurements is similar to the one described for the calibration (Fig. 5). First, the transient thermal response measured by the fluxmeter is recorded until steady state is reached. Second, the flow is stopped. At last, the thermal response, corresponding to the decrease of the temperature, is recorded. For all the experiments, the stoichiometric proportions are applied. The measured heat flux can be described by Eq. (5).

$$\phi = \Delta H_r Q C X \tag{5}$$

where ϕ is the heat flux (W), ΔH_r is the enthalpy ($\mathrm{J\,mol^{-1}}$), Q is the flow rate ($\mathrm{L\,s^{-1}}$), C is the concentration ($\mathrm{mol\,L^{-1}}$) and X is the conversion rate. Because the reaction is completed, the heat flux released by the reaction is directly proportional to the molar flow rate. Thus, the reaction must be complete ($X = 1$) in the microreactor. For this reason, the residence time has to be longer than the reaction one. As the plot of the heat flux versus the molar flow rate provides a line the reaction is complete in the microfluidic chip.

3.1.1. Sensitivity of the enthalpy determination

The enthalpy is determined by the use of the microcalorimeter. During experiments, the global heat flux produced by the chemical reaction is measured. As the molar flow rate is known, the reaction enthalpy can be deduced from Eq. (6).

$$\Delta H_r = \frac{\phi}{QCX} = \frac{\alpha U}{QCX} \tag{6}$$

where Q is the flow rate of the limiting reagent ($\mathrm{L\,s^{-1}}$), C is the concentration of the limiting reagent ($\mathrm{mol\,L^{-1}}$), ΔH_r is the reaction enthalpy ($\mathrm{J\,mol^{-1}}$), X is the conversion rate, α is the calibration coefficient ($\mathrm{W\,V^{-1}}$) and U is the measured tension (V).

According to Eq. (6), the standard deviation of estimated enthalpy depends on the flow rate (Q), the numerical voltmeter (U) and the calibration coefficient (α). As the chemical reaction is complete in the microfluidic chip, the conversion X is equal to 1. The solutions are commercial solutions and the standard error of the concentration is negligible (7×10^{-2}%).In order to estimate the error of each parameter, several experiments are realised.

- Firstly, the standard error of the injected flow rate is determined by a specific experiment. Some fluorinated oil is injected by the syringe pump and the weight of oil is measured as a function of time. Three different flow rates are tested: 100, 500 and 1500 $\mu\mathrm{L\,h^{-1}}$. This experiment is realised 20 times at each flow rate

Table 1
Experimental and manufacturer values of the calibration coefficient: α.

Temperature (°C)	Experimental coefficient ($\mathrm{W\,V^{-1}}$)	Manufacturer coefficient ($\mathrm{W\,V^{-1}}$)	$\alpha_{experimental}/\alpha_{manufacturer}$
25	3.95	3.14	1.26
50	3.74	3.10	1.21
80	3.98	3.1	1.29

Table 2
Results of the standard error of the calibration coefficient for different temperatures.

Temperature (°C)	25	50	80
Average of calibration coefficient α ($\mathrm{W\,V^{-1}}$)	3.95	3.74	3.98
Standard deviation σ ($\mathrm{W\,V^{-1}}$)	1.10^{-3}	4.10^{-3}	5.10^{-3}
Relative error u_α (%)	0.025	0.11	0.13

Table 3
Results of the enthalpy sensitivity.

	$u_{experimental}$ (%)	$u_{setting}$ (%)	$u_{relative}$ (%)
$Q_{theoretical} = 100\,\mu L\,h^{-1}$	2.17	2.52	4.69
U for $P = 100$ mW	0.028		0.028
α	0.025		0.025

that determines the experimental standard error ($u_{experimental}$) defined by Eq. (4). The experimental flow rate is then compared to the theoretical flow rate and the setting error ($u_{setting}$) is obtained (Eq. (7)). The highest error is used to calculate the error on the enthalpy estimation and is relative to the flow rate of 100 μL h^{-1}.

$$u_{setting} = \frac{Q_{theoretical} - Q_{experimental}}{Q_{theoretical}} \quad (7)$$

- Secondly, the accuracy of the measured tension is estimated by the experimental error and the reading error (10^{-3} mV). We apply various power by the use of the calibration chip to determine the experimental error. This experiment is performed 30 times for the three different power: 200, 600, and 1000 mW. Thus the experimental error is determined. The highest error on the measured tension is used to calculate the error on the enthalpy estimation.
- Finally, the relative error of the calibration coefficient has been evaluated previously.

The results are presented in Table 3. The sum of these results leads to the error on the experimental enthalpy of reaction which is estimated at 4.7%.

3.1.2. Monophasic flow

We study the acid–base reaction with one liquid phase flow: co-flow. This experiment is performed at Ts = 25 °C for several flow rates ranging from 250 to 1250 μL h^{-1}. In microfluidic device, the Reynolds number is very low (<1), so the flow is laminar. The reagents mixing is realised by diffusion. Measurements performed by an infrared camera allow us to show that the reaction occurs at the interface between the two reagents (Fig. 7). The interdiffusion area was measured and studied by several investigations and leads to estimate the mixing time [15–17].

The solution of Eq. (8) gives the concentration profile of a solute which diffuses in a microchannel.

$$\frac{\partial C}{\partial t} + \bar{U}\nabla C = D\nabla^2 C \quad (8)$$

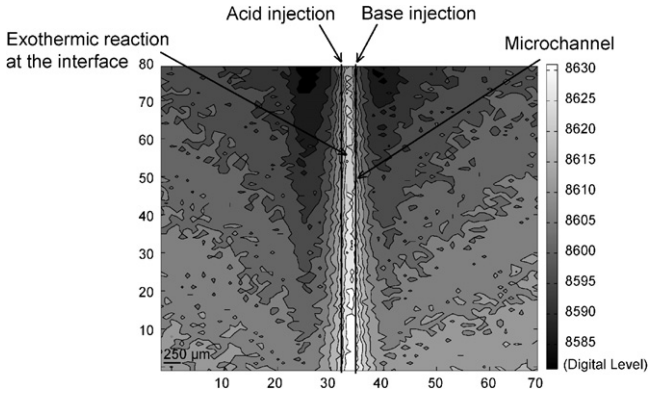

Fig. 7. Infrared image of acid–base reaction co-flow in a microchannel of 250 μm width, the white colour corresponds to the highest temperature and the black one to the coldest temperature.

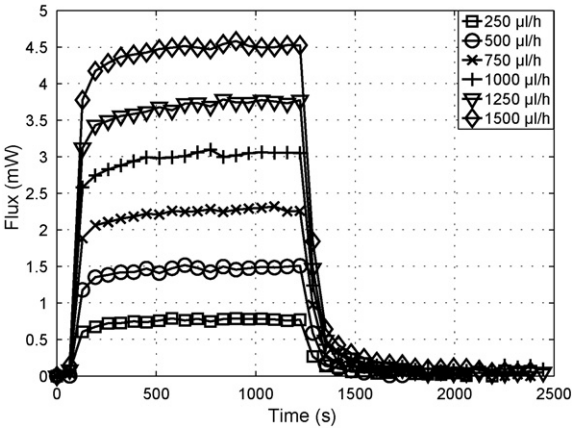

Fig. 8. The measured heat flux is represented versus time for different reagent flow rates in co-flow at Ts = 25 °C; one point over 500 is drawn.

The diffusion length, which corresponds to the mixing length X_m, can be described by Eq. (8).

$$\sigma = \sqrt{2Dt} = \sqrt{2D\frac{X_m}{U}} \rightarrow X_m = \frac{1}{8}\frac{w^2 U}{D} \quad \text{with}$$

$$P_e = \frac{wU}{D} \rightarrow X_m = \frac{1}{8}P_e w \quad (9)$$

where σ is the half width of the diffusion cone (m), D is the diffusion coefficient (m^2 s^{-1}), C is the concentration (mol m^{-3}), U is the flow velocity (m s^{-1}), X_m is the diffusion length (m), t is the time (s), w is the channel width (m) and P_e is the Peclet number.

We use a microchannel of 250 μm width, the flow rate varies from 500 to 2500 μL h^{-1} thus the mixing length goes from 17 to 90 mm. As the length of the microchannel is 32 cm the reagents are fully mixed inside the chip. The acid–base reaction is a fast reaction thus the reaction is complete inside the chip and the conversion rate is equal to 1.

During experiments, the heat flux produced by the chemical reaction in the microcalorimeter is recorded as a function of time at various flow rates, as it is represented in Fig. 8.

Then the heat flux released by the reaction is compared to the molar flow rates. The evolution is linear. By Eq. (5) the slope gives directly the reaction enthalpy (Fig. 9).

The value of the enthalpy we obtained is 54.38 ± 2.78 kJ mol^{-1} with an estimated uncertainty of 5.13%. This value corresponds to the value of 55.8 kJ mol^{-1} provided by the literature [18] with a deviation lower than 3%.

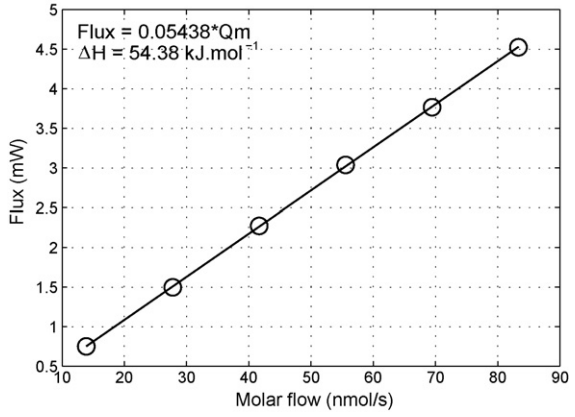

Fig. 9. Heat flux versus molar flow rates in co-flow at Ts = 25 °C; solid line correspond to the linear regression and the linear relation allows to determine the reaction enthalpy.

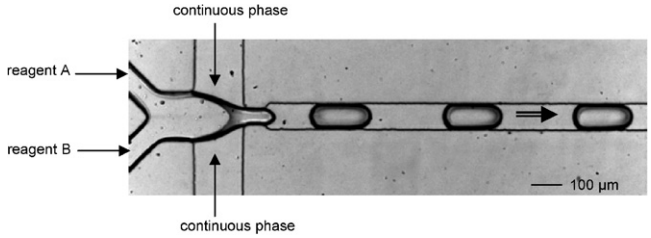

Fig. 10. Droplets formation mechanism in a flow-focusing junction.

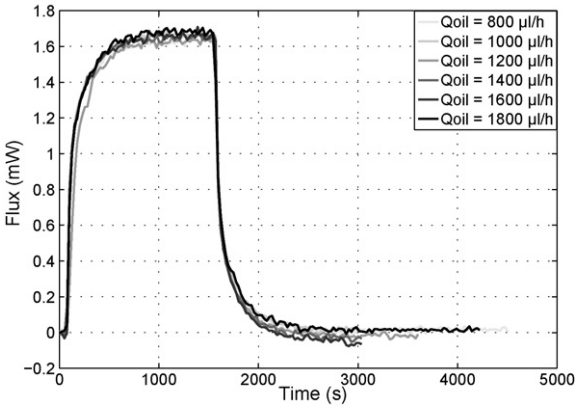

Fig. 11. Measured heat flux versus time at constant reagents flow rate and various oil flow rates in droplets flow at Ts = 25 °C; as the different curves are overlapped the oil has no influence on the heat flux measured.

3.1.3. Biphasic flow (droplets)

We used the so called "flow focusing" geometry to engineer aqueous droplets in oil within microchannels. Fig. 10 illustrates the microfluidic pattern of the flow focusing geometry designed for the experiment. In this channel geometry two oil inlets and two aqueous inlets are forced to flow through a channel restriction located downstream the junction resulting in the formation of aqueous droplets. We use silicone oil with a viscosity of 20 mPa s as the inert continuous flow and the chemical reaction occurs in the droplets (microreactors).

Two different sets of experiments are carried out.

Firstly, the droplets volume is changed by variation of oil flow rate with a constant reagents flow rate. As the reagent flow rate is constant, the reagent quantity introduced in the microcalorimeter is constant and the heat produced by the chemical reaction should be the same. Fig. 11 represents the heat released by the chemical reaction, which is the same for all oil flow rates. Thus we can assume that the oil flow rate has no effect on the heat measurement in this device and the droplet flow can be performed.

Secondly, the total flow rate is varied while the ratio between the reagents flow rate and the oil flow rate is constant and equal to 0.5. Then the reaction enthalpy can be estimated as previously (Fig. 12). The reaction enthalpy is estimated at $55.74 \pm 2.86\ \mathrm{kJ\ mol^{-1}}$. This value is in good agreement with the literature value of $55.8\ \mathrm{kJ\ mol^{-1}}$, the deviation is about 0.1% [18]. This result is close to the value determined by this microcalorimeter in co-flow.

3.2. Characteristic mixing time

In this study, reagents are introduced in co-flow. As it has been explained in Section 3.1.2, in such device the reagents mixing is performed by species diffusion. The strong acid–base reaction is a very fast reaction, thus chemical reaction is limited by the species diffusion.

In order to study the conversion rate, the reaction should not be totally achieved inside the microreactor. The residence time has to be lower than the reaction time. Therefore a specific microfluidic chip is designed with a volume of 16 nL, 100 µm width, 80 µm depth and 2 mm length.

The acid–base reaction is studied in the microcalorimeter at different flow rates from 200 to 1000 $\mu\mathrm{L\ h^{-1}}$ (Fig. 13), and in stoichiometric ratio at Ts = 5 and 25 °C.

As the enthalpy reaction has been determined (cf. Section 3.1.2), the heat flux is measured and the flow rate is known, the conversion rate is determined by Eq. (5) and plotted versus the residence time for different temperatures (Fig. 14).

In Fig. 14, we can observe that the species diffusion is faster at high temperature. Concerning experiments at room temperature, the mixing time is estimated about 0.145 s, for $X = 0.95$. The apparent diffusion coefficient can be calculated using Eq. (9): $D = (1/8)(w^2/t)$, thus D is estimated at $8.6 \times 10^{-9}\ \mathrm{m^2\ s^{-1}}$. This value is in agreement with the diffusion coefficient of H^+ in water which is about $9.3 \times 10^{-9}\ \mathrm{m^2\ s^{-1}}$ [19].

3.3. Calorimetric titration

We use the microfluidic chip designed for the enthalpy measurement to perform the titration experiment. A NaOH solution with a concentration of $0.2\ \mathrm{mol\ L^{-1}}$, is considered as the unknown concentration solution. This NaOH solution is titrated by a HCl solution. The concentration of this HCl solution is well known

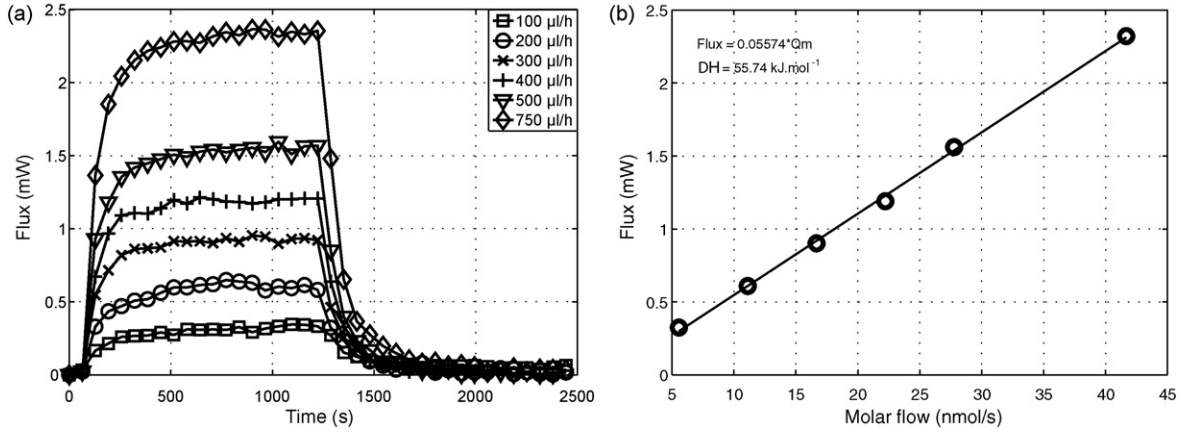

Fig. 12. (a) Measured heat flux versus time with constant ratio (reagent flow rate over oil flow rate) in droplets flow at Ts = 25 °C; one point over 500 is drawn and (b) heat flux with constant ratio (reagent flow rate over oil flow rate) versus the reagent molar flow rates in droplets flow at Ts = 25 °C; solid line corresponds to the linear regression and the linear relation allows to determine the reaction enthalpy.

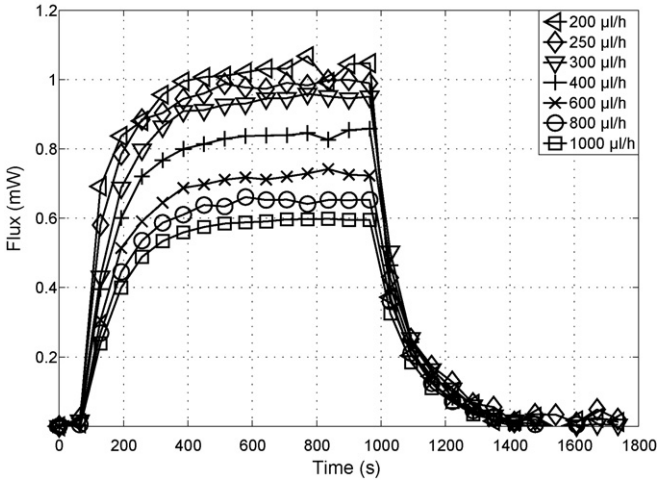

Fig. 13. Relative measured heat flux versus time in co-flow at Ts = 5 °C for different reagents flow rates; the relative heat flux is the ratio of the measured heat flux over the theoretical heat flux produced if the reaction is completed in the reactor.

and equal to 0.1 mol L^{-1}. The experiments come out the following way: the NaOH flow rate is constant and equal to 400 µL h^{-1}, then the HCl flow rate increases until the measured heat flux reaches a constant value. The reaction occurs in stoichiometric ratio when the heat flux steady state is reached. Thus, the equivalent flow rate is determined at the beginning of this steady state. The increase of the HCl flow rate is done in two different ways: firstly it increases steadily each 15 min until reaching the steady state (Fig. 15(a)); secondly, as it is shown in Fig. 15(b), the flow rate of HCl increases continuously each minute.

According to the two sets of experiments, the maximum heat flux is measured when the HCl flow rate is equal to 800 µL h^{-1}. So the stoechiometry of the chemical reaction is obtained at the expected value of the NaOH concentration (i.e. 0.2 mol L^{-1}).

3.4. Mixing and reaction enthalpy of an esterification reaction

We have chosen to study the homogenous esterification reaction between propionic anhydride and 2-butanol (Eq. (10)). This reaction is investigated in the literature relative to process safety and some thermokinetic parameters are available [20,21].

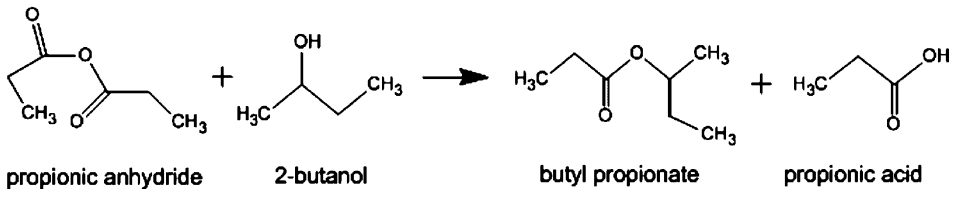

(10)

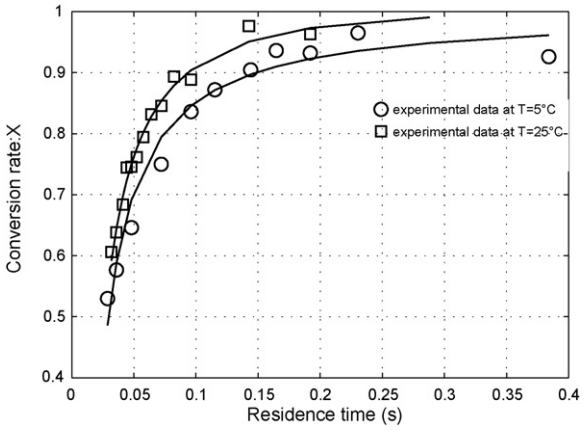

Fig. 14. Conversion rate versus residence time at different setting temperatures (Ts).

This reaction is known to be a second order reaction, it is first order in each reagent. The time of the reaction is quite slow; indeed the reaction is complete after 20 h at 70 °C. However a catalyst (such as sulphuric acid) is used to reduce the reaction time. For example, the reaction is completed after 2 h and 30 min at 30 °C with the use of sulphuric acid at 3% (molar) in 2-butanol.

In order to measure the enthalpy of the reaction, it is relevant to first determine the enthalpy of the mixing. It is found in the literature [21] that the enthalpy of mixing is endothermic and has a value of −4.2 kJ mol^{-1}, which is not insignificant.

3.4.1. Mixing enthalpy

During these experiments, the mixing of the reagents (propionic anhydride and 2-butanol) is performed in stoichiometric proportions, in the microfluidic chip without catalyst. As the residence time is kept lower than 10 min, the reaction has not begun in the microreactor. Thus the measured heat flux corresponds to the enthalpy of the reagents mixing. Two sets of experiments are realised.

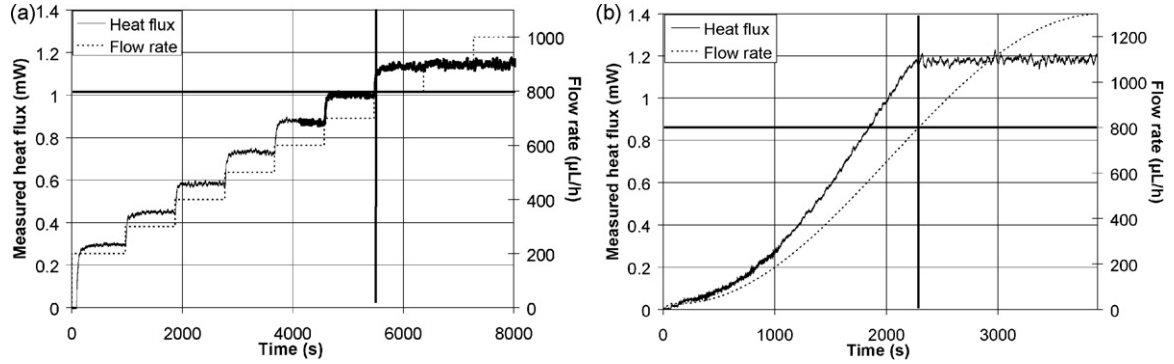

Fig. 15. Measured heat flux versus time at different flow rates at Ts = 25 °C for calorimetric titration of NaOH solution (0.2 mol L^{-1}) by HCl solution (0.1 mol L^{-1}): (a) flow rate of HCl changes each 15 min and (b) flow rate of HCl changes each 60 s.

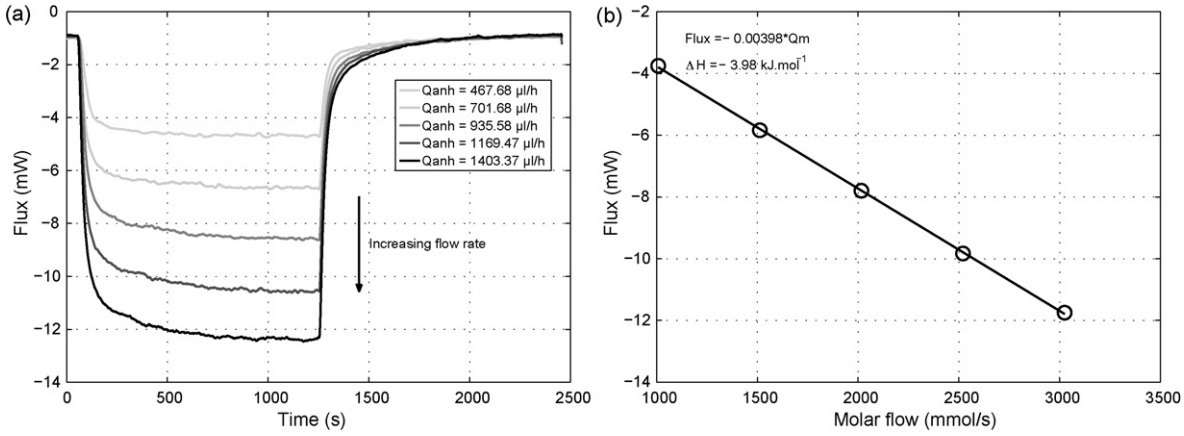

Fig. 16. Determination of the mixing enthalpy of the esterification reaction in co-flow at Ts = 30 °C: (a) measured heat flux versus time at various flow rates and (b) heat flux versus the reagent molar flow rates, solid line corresponds to the linear regression.

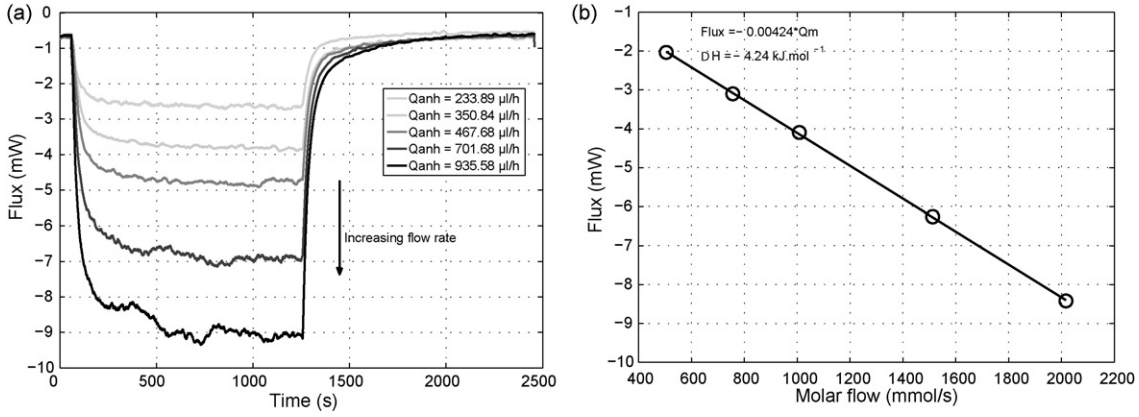

Fig. 17. Determination of the mixing enthalpy of the esterification reaction in droplets at Ts = 30 °C: (a) measured heat flux versus time at various flow rates and (b) heat flux versus the reagent molar flow rates, solid line corresponds to the linear regression.

Firstly, the mixing enthalpy is determined in co-flow, the results are presented in Fig. 16. The heat flux measured is negative (Fig. 16(a)) and increase with the flow rate. Thus the mixing enthalpy is an endothermic phenomenon. According to the Fig. 16(b), the experimental enthalpy of mixing is $-3.98 \pm 0.2\ \mathrm{kJ\,mol^{-1}}$. The deviation of this value compared to the literature value ($\Delta H_m = -4.2\ \mathrm{kJ\,mol^{-1}}$) is 5.3% which is sufficiently good [21].

The second set of experiment is relative to the measurement of the mixing enthalpy in droplets. The inert continuous flow in made of a fluorinated oil with a viscosity of 10 mPa s. The results obtained are shown in Fig. 17. We can also observe that the heat flux is negative which means that the enthalpy due to the mixing corresponds to an endothermic phenomenon. The plot of the heat flux versus the molar flow rate, the mixing enthalpy is estimated at $-4.24 \pm 0.22\ \mathrm{kJ\,mol^{-1}}$ that is very close to the literature [21].

3.4.2. Reaction enthalpy

In order to estimate the enthalpy of reaction, the chemical reaction must be complete in the microfluidic chip. The sulphuric acid is used as a catalyst and is diluted in the 2-butanol at 3% (molar fraction to 2-butanol). The temperature is set at 30 °C and the reaction is completed after 2 h and 30 min. Consequently the maximum total flow rate should be $50\ \mu\mathrm{L\,h^{-1}}$ in the microfluidic chip (channel volume is 117 µL). The reagents are introduced in co-flow in stoichiometric ratio. Therefore the heat flux measured is the result of the mixing process and the reaction. As the mixing enthalpy is lower than the reaction enthalpy, the results show only an exothermic phenomenon.

The plot of the heat flux versus the molar flow rate is linear and allows to determine the global enthalpy (Fig. 18). The estimated value is $\Delta H_{exo} = 54.8\ \mathrm{kJ\,mol^{-1}}$.

As the mixing enthalpy (ΔH_{endo}) is known, the enthalpy of reaction (ΔH_r) can be determined using Eq. (11).

$$\Delta H_r = \Delta H_{exo} - \Delta H_{endo} \tag{11}$$

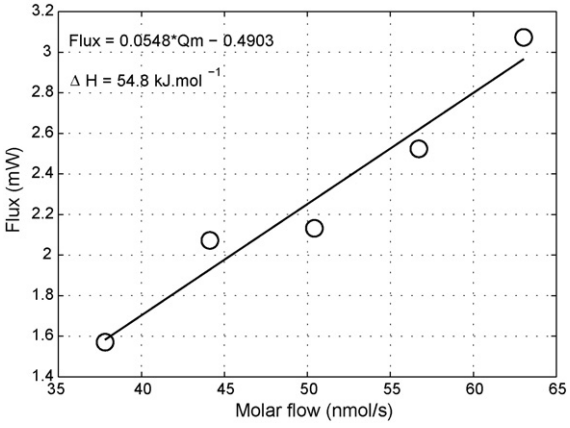

Fig. 18. Determination of the reaction enthalpy of the esterification reaction in co-flow at Ts = 30 °C: heat flux versus the reagent molar flow; solid line corresponds to the linear regression and the linear relation allows to determine the reaction enthalpy.

Thus, the experimental enthalpy of the reaction is $58.78 \pm 3\,kJ\,mol^{-1}$, which is close to the literature value ($62.5 \pm 1\,kJ\,mol^{-1}$) with a deviation of 6% [20,21].

4. Conclusion

A microfluidic calorimeter under continuous flow has been developed and validated for the measurements of titration, kinetic, mixing and reaction enthalpy of chemical reaction. In this paper, a validation on the characterization of a strong acid–base chemical reaction was performed. The experimental results obtained are very close to the values found in the literature (<5%). This isothermal microcalorimeter allows chemical characterizations (enthalpy, conversion rate, and titration) in droplets and co-flow. The droplets flow is very useful in case of very high exothermic reaction because of the important ratio between surface and volume. In fact, such ratio provides a very low temperature increases. These advantages are very interesting for safety studies.

To summarize, the main advantages of the device are the followings:

- The manufacturing of microfluidic chips makes it possible to obtain isothermal conditions with various geometries of reactor (sizes and volumes).
- The fluxmeter offers a good sensitivity and a direct measurement of heat flux. The thermopiles are independent of the chip and not very expensive. Working in steady state removes all problems involved in its inertia.
- With the injection system, it is possible to investigate a large range of residence times and concentrations.
- The required time to estimate the reaction enthalpy is around 2 h, which is very short.

Finally, this device could be coupled to an infrared camera in order to perform local chemical analysis [22]. The use of both methods will allow the study of various chemical reactions in order to obtain thermochemical data.

References

[1] A. Zoog, F. Stoessel, U. Fisher, K. Hungerbühler, Isothermal reaction calorimetry as a tool for kinetic analysis, Thermochim. Acta 419 (2004) 1–17.
[2] P. Tabeling, Introduction à la Microfluidique, Collection Echelles, Belin, 2003.
[3] J.M. Köhler, M. Zieren, Chip reactor for microfluidic calorimetry, Thermochim. Acta 310 (1997) 25–35.
[4] H. Ernst, A. Jachimowicz, G.A. Urban, High resolution flow characterization in Bio-MEMS, Sens. Actuators A 100 (2002) 54–62.
[5] M.A. Schneider, T. Maeder, P. Ryser, F. Stoessel, A microreactor-based system for the study of fast exothermic reactions in liquid phase: characterization of the system, Chem. Eng. J. 101 (2004) 241–250.
[6] J. Lechner, A. Wolf, G. Wolf, V. Baier, E. Kessler, M. Nietzsch, M. Krügel, A new micro-fluid chip calorimeter for biochemical applications, Thermochim. Acta 445 (2006) 144–150.
[7] D. Ross, M. Gaitan, L.E. Locascio, Temperature measurement in microfluidic systems using a temperature-dependant flurorescent dye, Anal. Chem. 73 (2001) 4117–4123.
[8] H.F. Arata, P. Löw, K. Ishizuka, C. Bergaud, B. Kim, H. Noji, H. Fujita, Temperature distribution measurement on microfabricated thermodevice for single biomolecular observation using fluorescent dye, Sens. Actuators B 117 (2006) 339–345.
[9] K.-P. Möllmann, N. Lutz, M. Vollmer, Thermography of Microsystems, Inframation 2004 Proceeding, ITC 104 A 2004-07-27.
[10] W. Ferstl, S. Loebbecke, J. Antes, H. Krause, M. Haeberl, D. Schmalz, H. Muntermann, M. Grund, A. Steckenborn, A. Lohf, J. Hassel, T. Bayer, M. Kinzl, I. Leipprand, Development of an automated microreaction system with integrated sensorics for process screening and production, Chem. Eng. J. 101 (2004) 431–438.
[11] C. Hany, C. Pradere, J. Toutain, J.-C. Batsale, A millifluidic calorimeter with infrared thermography for the measurement of chemical reaction enthalpy and kinetics, QIRT J. 5 (2) (2008) 211–229.
[12] J.C. Bastsale, C. Pradere, M. Joanicot, J. Toutain, C. Gourdon, Procédés de détermination d'au moins un paramètre d'une transformation physique et/ou chimique, dispositif et installation correspondants, French Patent, 2897156 (2006).
[13] O. Fudym, C. Pradere, J.C. Batsale, An analytical two-temperature model for convection-diffusion in multilayered systems: application to the thermal characterisation of microchannel reactors, Chem. Eng. Sci. 62 (15) (2007) 4054–4064.
[14] D. Maillet, S. Andre, J.C. Bastsale, A. Degiovanni, C. Moyne, Thermal Quadrupoles: Solving the Heat Equation through Integral Transforms, Wiley and Sons, 2000.
[15] A.E. Kamholz, B.H. Weigl, B.A. Finlayson, P. Yager, Quantitative analysis of molecular interaction in a microfluidic channel: the T-sensor, Anal. Chem. 71 (1999) 5340–5347.
[16] R.F. Ismagilov, D. Rosmarin, P.J.A. Kenis, D.T. Chiu, W. Zhang, H.A. Stone, G.M. Whitesides, Pressure-driven laminar flow in tangential microchannels: an elastomeric microfluidic switch, Anal. Chem. 73 (2001) 4682–4687.
[17] J.B. Salmon, C. Dubrocq, P. Tabeling, S. Charier, D. Alcor, L. Jullien, F. Ferrage, An approach to extract rate constants from reaction—diffusion dynamics in a microchannel, Anal. Chem. 77 (2005), 3417-3224.
[18] D.R. Lide, Handbook of Chemistry and Physics, 72nd ed., CRC Press, 1991–1992, pp. 1–5.
[19] J. Newman, Electrochemical Systems, 2nd ed., Prentice-Hall, Englewood Cliffs, NJ, 1991.
[20] O. Ubrich, B. Srinivasan, P. Lerena, D. Bonvin, F. Stoessel, Optimal feed profile for a second order reaction in a semi-batch reactor under safety contraints, experimental study, J. Loss Prev. Process Indust. 12 (1999) 485–493.
[21] W. Benaissa, Développem ent d'une méthodologie pour la conduite en sécurité d'un réacteur continu intensifié, in: étude de l'estérification de l'anhydride propionique par le 2-Butanol, Institut National polytechnique de Toulouse, décembre 2006 (Chapitre 2).
[22] C. Pradere, M. Joanicot, J.C. Batsale, J. Toutain, C. Gourdon, Processing of temperature field in chemical microreactors with infrared thermography, Quant. InfraRed Thermogr. 3 (1) (2006) 117–135.